

SLOW POSITRON STUDIES OF HYDROGEN ACTIVATION/
PASSIVATION ON SiO₂/Si(100) INTERFACES

K.G. Lynn and P. Asoka-Kumar
Brookhaven National Laboratory, Upton, New York, 11973.

The hydrogen atoms are one of the most common impurity species found in semiconductor systems owing to its large diffusivity, and are easily incorporated either in a controlled process like in ion implantation or in an uncontrolled process like the one at the fabrication stage. Hydrogen can passivate dangling bonds and dislocations in these systems and hence can be used to enhance the electrical properties.^{1,2} In a SiO₂/Si system, hydrogen can passivate electronic states at the interface and can alter the fixed or mobile charges in the oxide layer. Since hydrogen is present in almost all of the environments of SiO₂/Si wafer fabrication, the activation energy of hydrogen atoms is of paramount importance to a proper understanding of SiO₂/Si based devices and has not been measured on the technologically most important Si(100) face. There are no direct, nondestructive method available to observe hydrogen injection into the oxide layer and subsequent diffusion. This study uses the positrons as a 'sensitive', nondestructive probe to observe hydrogen interaction in the oxide layer and the interface region. We also describe a new way of characterizing the changes in the density of the interface states under a low-temperature annealing using positrons

When energetic positrons are implanted into solids, they rapidly thermalize (1-10 ps) through various energy loss processes and annihilate with electrons, predominantly producing two photons of 511 keV. Since the thermalized positrons have much lower momenta than their annihilation partners, the Doppler shift of the γ -ray is determined by the initial state of the many-electron system at the annihilation site. The Doppler broadening of the annihilation photopeak will be quantified using the standard S (for shape) parameter.³ The details of the experimental setup used for the present study are described elsewhere.^{4,3} The positron beam intensity during this measurement was $\sim 5 \times 10^5$ e⁺/s, too low to produce any measurable radiation damage. The annihilation γ -rays are recorded in a Ge detector.

The SiO₂/Si wafers had an n-type, (100) substrate with a 100 nm thick oxide layer grown by Plasma Enhanced Chemical Vapour Deposition (PECVD) and a 110 nm oxide layer grown by thermal process (dry/no HCl). The wafers were not subjected to a post oxidation anneal. The sample was annealed in the experimental chamber at various stages as explained later. The hydrogen exposure amounted to 1.6×10^6 Langmuir (1L = 10⁻⁶ torr-sec).

The experiment was performed at incident energies of 0.4 to 20.4 keV in steps of 0.25 keV. The S-parameter is evaluated for each incident energy resulting in a S-parameter versus energy curve, called S-E curve. A typical S-E curve for a SiO₂/Si system is shown in Fig. 1. The solid line through the data points correspond to a fit to the theoretical model described elsewhere.³

The data shows distinct signals corresponding to surface, oxide, interface, and bulk silicon.

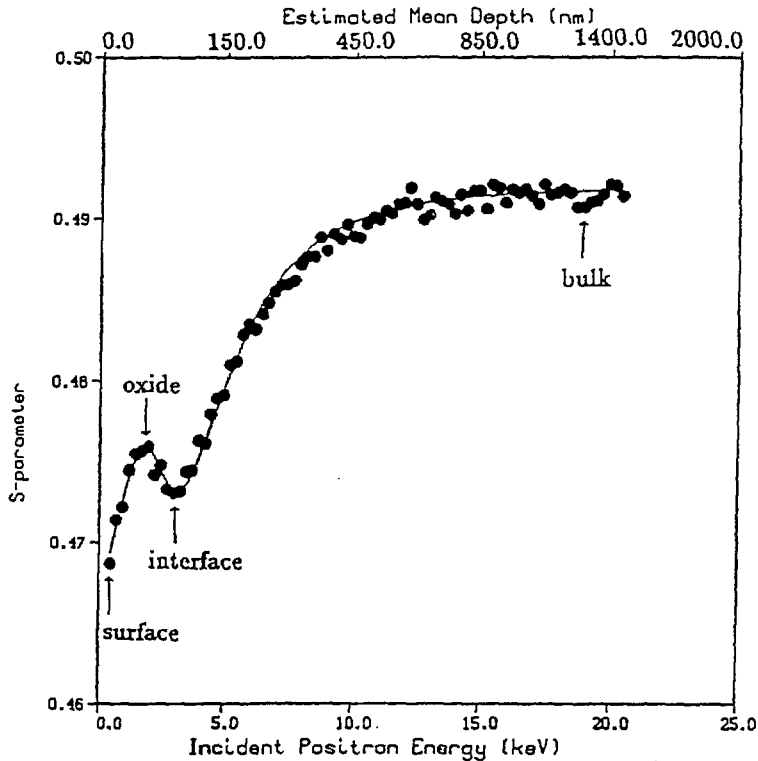


Fig. 1 A typical S-parameter vs energy (E) measurements for SiO_2/Si system. The figure shows distinct S-parameter values corresponding to the oxide, interface, and bulk $\text{Si}(100)$.

what do you think??

A normalized S-parameter, defined as the ratio of the S-parameter for a given energy value to the S-parameter corresponding to the bulk silicon, will be used to reduce any systematic errors between different set of measurements or experimental arrangements. The bulk S-parameter (denoted by S_b) is obtained by averaging the S-parameter values for incident positron energies higher than 15.0 keV.

The incident positron energy is directly related to the mean penetration depth and can be approximated by a power law.³ The mean penetration

depth \bar{z} at a given energy E is given by

$$\bar{z} = AE^n, \quad (1)$$

where $A = (332/\rho) (\text{\AA}/\text{keV}^n)$, $n \sim 1.7$, and E is the beam energy in keV.⁵ Here ρ stands for the mass density of the material. In this article Eq. (1) will be used to convert incident positron energies to mean penetration depths. By varying the positron energy, one can probe the SiO_2/Si system at different depths. Here, we will mostly concentrate on incident energies of 1.0-3.0 keV

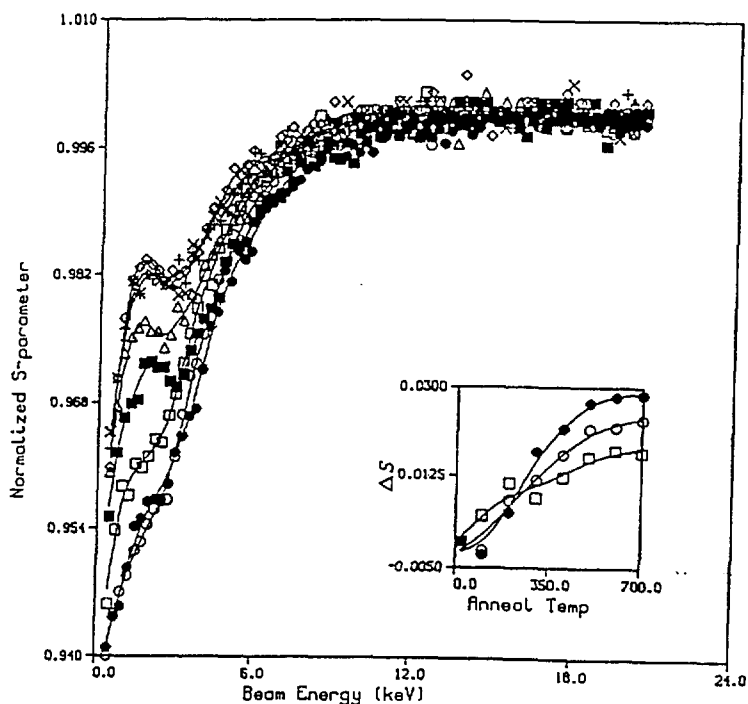


Fig. 2 The S-parameter curves corresponding to annealing at successively increasing temperatures in steps of 100 °C. All measurements are performed at room temperature. Symbols denote: (●) 20°C, (○) 100°C, (□) 200°C, (■) 300°C, (△) 400°C, (+) 500°C, (×) 600°C, and (◇) 700°C. The insert shows the change in S-parameter as a function of the anneal temperature for four different energies which is generated using the S-E curves. Symbols in the insert denote: (●) 1.7 keV, (○) 2.7 keV, and (□) 3.7 keV.

corresponding to the oxide layer and energies of ~ 4.0 keV corresponding to the interface region. The energies 1.0, 3.0, and 4.0 keV correspond to mean penetration depths of ~ 15 , ~ 65 , and ~ 100 nm, respectively.

In Fig. 2, a series of normalized S-E curves are shown corresponding to different annealing temperatures. All the measurements are performed at room temperature ($\sim 20^\circ\text{C}$). The straight line through these data points are drawn as a guide to the eye. The normalized S-parameter corresponding to the oxide layer increases with the annealing temperatures and saturates at $\sim 500^\circ\text{C}$. A similar behaviour is evident at the interface, although the size of the change is smaller. The insert in Fig. 2 shows the change in the normalized S-parameter (denoted by ΔS) for three different incident energies, 1.7 keV, 2.7 keV, and 3.7 keV, as a function of annealing temperatures

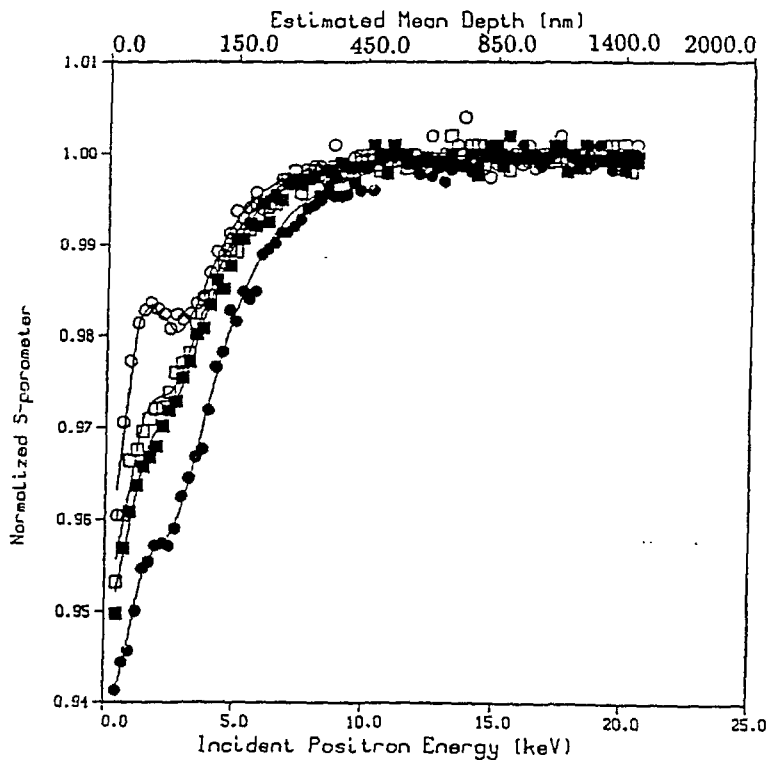


Fig. 3 S-E curves corresponding to (●) first room temperature measurement before the start of the anneal cycle, (○) after annealing at 700°C , (□) after annealing at 700°C and exposure to hydrogen at room temperature, and (■) after annealing at 700°C and subsequent cooling in hydrogen ambient. All measurements are performed at room temperature.

and is obtained from the raw data sets in the main figure. The changes in the normalized S-parameters are evaluated with respect to the first room temperature measurement (i.e. before the start of the annealing cycles).

The sample was exposed to atomic hydrogen after each annealing cycle to test if the changes observed in Fig. 2 are associated with hydrogen. In order to obtain a consistent picture from hydrogen exposure effects as opposed to other thermally activated processes, an S-E scan was performed in the following order whenever the annealing temperature is raised to a new value: room temperature, annealing temperature, room temperature, hydrogen exposure at room temperature, back upto same annealing temperature, and room temperature. Each annealing was performed for a duration of ~ 6 hours and subsequent cool down to room temperature lasted for a period of ~ 2 hours. The 6 hour annealing time is chosen to accommodate the S-E measurement at the annealing temperature. Fig. 3 shows four sets of data points corresponding to the first room temperature measurement, room temperature measurement after annealing at ~ 700 °C in vacuum, room temperature measurement after the last step and subsequent hydrogen exposure at room temperature, and room temperature measurement after annealing at 700 °C and cooling down the sample in a hydrogen ambient. It is clear from these figures that part of the changes that are associated with the annealing can be recovered with hydrogen exposure. It was also found that the recovery of the system by hydrogen exposure can be reversed by repeating the annealing cycle.

The hydrogen activation energy can be evaluated using the results shown in the insert of Fig. 2. Consider a series of annealing at equally spaced temperatures, $T_0, T_1, T_2, \dots, T_i, \dots$ of duration τ sec. The hydrogen content $\mathcal{N}_H(i)$ at the beginning of the i^{th} cycle can be written as⁶

$$\frac{d\mathcal{N}_H(i)}{dt} = -\mathcal{N}_H(i)K_0 \exp\left(-\frac{\mathcal{E}}{k_B T_i}\right), \quad (2)$$

where K_0 is the vibrational frequency, \mathcal{E} is the activation energy, and k_B is the Boltzman constant. In writing Eq. (2) the annealing process is assumed to be of first order. Now assuming that the S-parameter is proportional to \mathcal{N}_H , the activation energy can be written as

$$\mathcal{E} \simeq k_B T_m \ln \left[\frac{K_0 \tau}{\ln\left(\frac{T_f - T_i}{T_i - T_f - 2\Delta T}\right)} \right], \quad (3)$$

where T_i and T_f are explained in Fig. 4. The parameter T_m is given by $T_m = \frac{T_i + T_f}{2}$ and ΔT is the step size in temperature. By substituting the appropriate numbers from Fig. 2 into Eq. 2 and assuming a vibrational frequency of 10^{13} s^{-1} , we deduce $\mathcal{E} = 2.02 \pm 0.07 \text{ eV}$. A similar value can also be obtained by a non-linear fitting procedure.

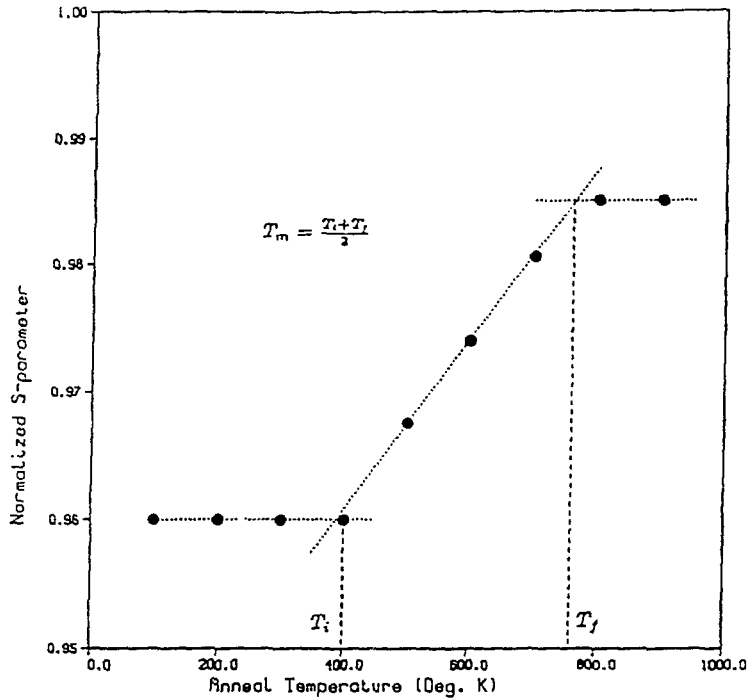


Fig. 4 A schematic diagram of S-parameter vs Temperature used for the evaluation of hydrogen activation energy.

In Fig. 5, the annealing behaviour of the different regions of the SiO_2/Si system with the thermally grown oxide are compared. The normalized S-parameter versus annealing temperature is plotted for mean penetration depths of 25, 110, 280, and 480 nm. The first two values mainly correspond to the overlayer and the interface and the last two values approach the bulk silicon value. The normalized S-parameter curves for the overlayer, represented by 25 nm data points, show only small changes under heating. However, the 110 nm curves, corresponding predominantly to the interface, shows a reduction in the normalized S-parameter for annealing temperatures from 100 to 400 °C. The 110 nm measurements and the low temperature annealing measurements for midgap interface trap density (D_{it}) performed with the CV-techniques (see ref. 1, p. 784, for details) show similar behaviour. This led us to identify the reduction of the normalized S-parameter with a decrease in the interface state density which can be understood as follows.

The thermalized positrons become localized to sites related to the interface states. A positron that annihilates from a trap site (which usually has more open volume⁷ for the positron to become localized) has a higher probability of encountering a slow moving electron than a freely diffusing positron. As a result, the annihilation photons from a trapped state will produce a sharper photon spectrum, i.e. a higher S-value. Hence, when the density of the interface states is reduced, the number of positrons annihilating from the specific trap sites is reduced, and this will in turn reduce the normalized S-parameter.

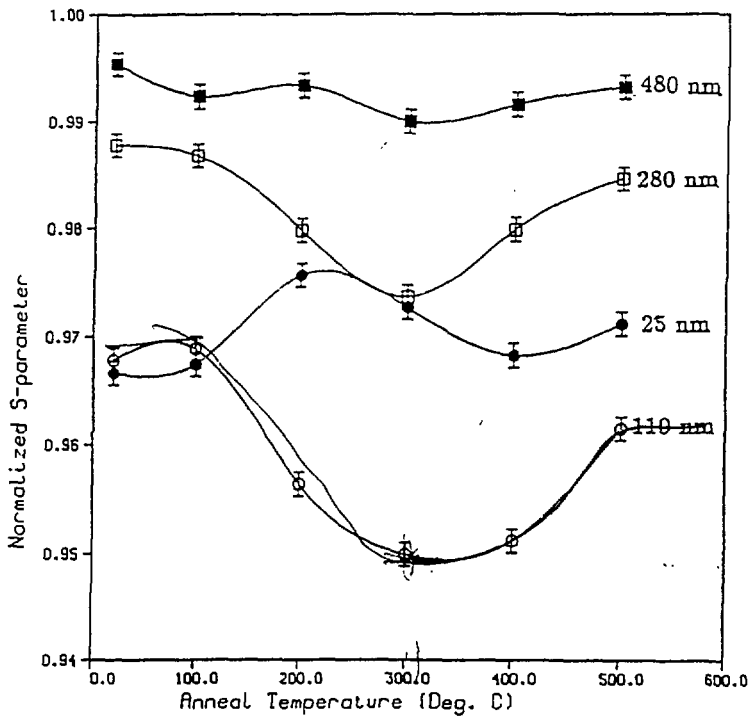


Fig. 5 The normalized S-parameter data as a function of annealing temperature for four mean implantation-depths, 25 nm, 110 nm, 280 nm, and 480 nm. The measurements are performed at the corresponding annealing temperatures. The 110 nm data set probe mainly the interface region and show a reduction for 100-400 °C. The lines through the data points are drawn as a guide.

The CV-measurement has established that the interface state densities in the SiO₂/Si system can be reduced by annealing at temperatures ranging from 200 to 400 °C.^{1,6} The exact annealing temperature that is required to produce the lowest interface state density varies depending on the processing method and annealing conditions of the wafer. If the sample is heated beyond 400 °C, the CV-method shows an increase in the interface state density. A similar trend for the normalized S-parameter curves corresponding to the interface region is shown in Fig. 5 (see curves for 110 nm).

The most obvious way to explain the changes at the interface is based on the activation-passivation of trap sites by hydrogen. It has been suggested that hydrogen is liberated from the oxide layer^{9,2} during annealing at around 300 °C. This hydrogen diffuses to the interface and passivates the trap sites. Hence positrons will encounter a reduced number of trap sites. This in turn can reduce the S-parameter as explained before. Beyond 400 °C, the captured hydrogen is again liberated from the interface region which causes a subsequent increase in the positron trap site concentration (i.e. interface states).

To test this scenario, a sample from the same wafer used in the above annealing series was exposed to atomic hydrogen. The sample was annealed to 500 °C in steps of 100 °C in vacuum (10⁻⁷ torr) for 15 minutes. After each step the sample was cooled down to room temperature slowly and an S-E scan was performed followed by atomic hydrogen exposure and a second S-E scan. Results from these measurements are shown in Fig. 6. The two set of points (joined by straight lines) correspond to S-parameter measurements at 110 nm. The top curve corresponds to measurements before hydrogen exposure and the bottom curve corresponds to measurements after hydrogen exposure. Two important features are evident from these figures. One is the reduction of the interface state density with annealing as shown in Fig 5. The second one, is the reversible changes in the S-parameter when exposed to hydrogen.

The reduction of the interface S-parameter under hydrogen exposure is consistent with a scenario in which the dangling bonds at the interface are passivated by hydrogen. Atomic hydrogen become attached to the dangling bonds, which may otherwise act as trap sites for positrons. If positrons are attached to defect sites, a sharper annihilation spectra is produced resulting in a higher S-value as explained before. Results in Fig. 6 thus demonstrate that the positrons and hydrogen are getting trapped at the same defect sites and the trap centers are similar to the open volume defects for positron trapping.

The positron profiling of the interfacial properties will become more sensitive for samples with thinner oxide layers, which is required for developing more compact device structures. When the positrons are implanted to the interface region through a thinner oxide layer, the stopping profile of the positrons will be narrower and therefore will be confined more to the interface region. Hence the fraction of positrons annihilating at the interface (i.e. sensitivity to interface sites) will increase with a thinner oxide layer and will result in a larger signal from the interface region.

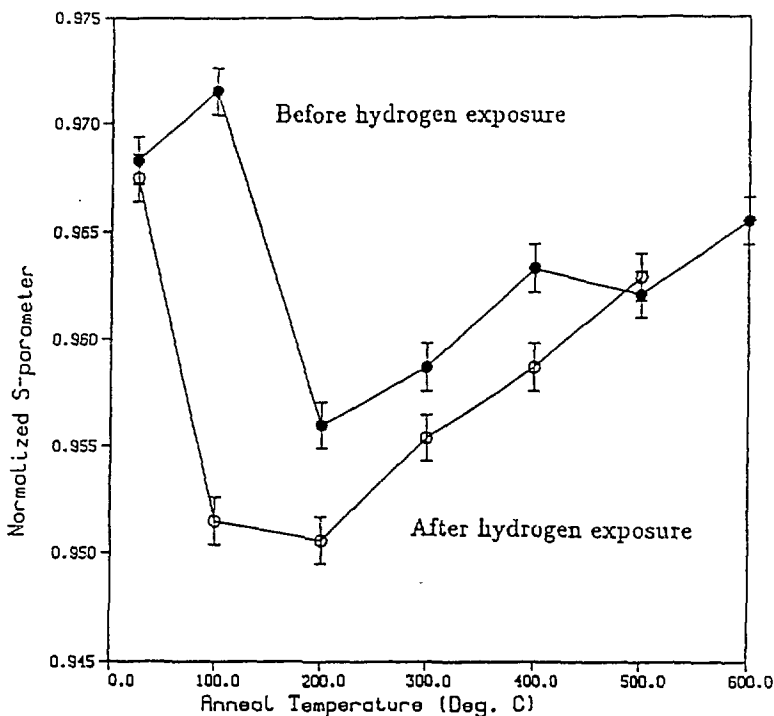


Fig. 6 S-parameter curves as a function of anneal temperature, before (upper curve) and after (lower curve) hydrogen exposure for 110 nm. All measurements are performed at room temperature.

In conclusion, we have shown that positron annihilation studies can be effectively employed to study the hydrogen activation and passivation of defect centers in an oxide-semiconductor structure. By repeated vacuum anneal and hydrogen exposure, the present study obtains the hydrogen activation energy for *technologically important Si(100)* face of an oxide system grown by PECVD process. On a thermally grown oxide structure, hydrogen is demonstrated to passivate interface state traps, which would otherwise trap positrons.

ACKNOWLEDGEMENT We thank T.C. Leung, B. Nielsen, Z.A. Weinberg and G. Rubloff for valuable discussions and for providing us with the samples used for the present investigations. This work is supported by US Department of Energy under contract No. DE-AC02-76CH00016.

REFERENCES

- 1) E.H. Nicollian and J.R. Brews, *MOS (Metal Oxide Semiconductor) Physics and Technology*, John Wiley & Sons, New York, (1982).
- 2) K.L. Brower, *Phys. Rev. B* **42**,3444(1990).
- 3) See for example, Peter J. Schultz and K.G. Lynn, *Rev. Mod. Phys.* **60**,701 (1988).
- 4) K.G. Lynn, B. Nielsen, and J.H. Quateman, *Appl. Phys. Lett.*, **47**,239 (1985).
- 5) P. Asoka-Kumar and K.G. Lynn, *Appl. Phys. Lett.* **57**,1634,(1990).
- 6) D.O. Welch, Private communication, (1989).
- 7) See for example: *Positrons in Solids*, ed. P. Hautojärvi, Springer-Verlag, New York, (1979).
- 8) Y.T. Yeow, D.R. Lamb, and S.D. Brotherton, *J. Phys. D: Appl. Phys.* **8**,1495(1975).
- 9) T. Fare, A. Špetz, M. Armgarth, and I. Lundström, *J. Appl. Phys.* **63**,5507 (1988).

DISCLAIMER

This report was prepared as an account of work sponsored by an agency of the United States Government. Neither the United States Government nor any agency thereof, nor any of their employees, makes any warranty, express or implied, or assumes any legal liability or responsibility for the accuracy, completeness, or usefulness of any information, apparatus, product, or process disclosed, or represents that its use would not infringe privately owned rights. Reference herein to any specific commercial product, process, or service by trade name, trademark, manufacturer, or otherwise does not necessarily constitute or imply its endorsement, recommendation, or favoring by the United States Government or any agency thereof. The views and opinions of authors expressed herein do not necessarily state or reflect those of the United States Government or any agency thereof.